Title
Long-Term Characterization of Axon Regeneration and Matrix Changes Using Multiple Channel Bridges for Spinal Cord Regeneration

Journal
Tissue Engineering Part A, 20(5-6)

ISSN
1937-3341

Authors
Tuinstra, Hannah M
Margul, Daniel J
Goodman, Ashley G
et al.

Publication Date
2014-03-01

DOI
10.1089/ten.tea.2013.0111

Peer reviewed

TISSUE ENGINEERING: Part A
Volume 20, Numbers 5 and 6, 2014

DOI: 10.1089/ten.tea.2013.0111

Long-Term Characterization of Axon Regeneration and Matrix Changes Using Multiple Channel Bridges for Spinal Cord Regeneration

Hannah M. Tuinstra, PhD,[1] Daniel J. Margul,[2] Ashley G. Goodman,[1] Ryan M. Boehler, PhD,[1] Samantha J. Holland,[1] Marina L. Zelivyanskaya,[1] Brian J. Cummings, PhD,[3,4] Aileen J. Anderson, PhD,[3,4] and Lonnie D. Shea, PhD[1,5–7]

Spinal cord injury (SCI) results in loss of sensory and motor function below the level of injury and has limited available therapies. The host response to SCI is typified by limited endogenous repair, and biomaterial bridges offer the potential to alter the microenvironment to promote regeneration. Porous multiple channel bridges implanted into the injury provide stability to limit secondary damage and support cell infiltration that limits cavity formation. At the same time, the channels provide a path that physically directs axon growth across the injury. Using a rat spinal cord hemisection injury model, we investigated the dynamics of axon growth, myelination, and scar formation within and around the bridge *in vivo* for 6 months, at which time the bridge has fully degraded. Axons grew into and through the channels, and the density increased overtime, resulting in the greatest axon density at 6 months postimplantation, despite complete degradation of the bridge by that time point. Furthermore, the persistence of these axons contrasts with reports of axonal dieback in other models and is consistent with axon stability resulting from some degree of connectivity. Immunostaining of axons revealed both motor and sensory origins of the axons found in the channels of the bridge. Extensive myelination was observed throughout the bridge at 6 months, with centrally located and peripheral channels seemingly myelinated by oligodendrocytes and Schwann cells, respectively. Chondroitin sulfate proteoglycan deposition was restricted to the edges of the bridge, was greatest at 1 week, and significantly decreased by 6 weeks. The dynamics of collagen I and IV, laminin, and fibronectin deposition varied with time. These studies demonstrate that the bridge structure can support substantial long-term axon growth and myelination with limited scar formation.

Introduction

Spontaneous regeneration of severed axons does not occur in the adult mammalian central nervous system (CNS). The failure to regenerate after injury is caused by a combination of factors, including inflammation, formation of the glial scar, release of myelin associated inhibitory factors, and an insufficient supply of growth promoting factors. However, CNS neurons are able to regrow when presented with a permissive environment.[1,2] Biomaterial scaffolds engineered to promote nerve regeneration, termed bridges, are able to provide a permissive environment for CNS regeneration. Bridges overcome barriers to regeneration by stabilizing the injury site, providing physical guidance for axons, preventing cavity formation, recruiting supportive cell types, and acting as a vehicle for the delivery of therapeutic factors or cells.[3–5]

The host response to spinal cord injury (SCI) is typified by limited endogenous repair[6–9] and is relatively slow.[10,11] By 2 weeks postinjury, contusion and compression injuries in rats result in a fluid-filled cavity[11] that expands rostrally and caudally from the epicenter with the onset of secondary injury and associated cell death.[12] A glial scar develops, which contains growth-inhibiting molecules that act as both physical and biochemical barriers to regeneration. A dense connective tissue scar composed of fibronectin, collagen fibers, laminin, Schwann cells, fibroblasts, and blood vessels also develops at the injury site.[10,13] Spared axons near the injury

Departments of [1]Chemical and Biological Engineering and [2]Biomedical Engineering, Northwestern University, Evanston, Illinois.
[3]Department of Physical Medicine and Rehabilitation, University of California, Irvine, California.
[4]Sue & Bill Gross Stem Cell Research Center, University of California, Irvine, California.
[5]The Robert H. Lurie Comprehensive Cancer Center of Northwestern University, Galter Pavilion, Chicago, Illinois.
[6]Institute for BioNanotechnology in Medicine and [7]Chemistry of Life Processes Institute, Northwestern University, Chicago, Illinois.

start demyelinating within 24 h of contusion with increasing demyelination out to 2 weeks.[10] Remyelination of spared axons by Schwann cells and oligodendrocytes through 22 weeks is limited.[14,15] Axons are rarely able to regenerate into the initially repaired tissue, are infrequently myelinated by Schwann cells, and form small bundles encased in fibroblasts.[10,11,16] Functional recovery after contusion injuries is mostly attributed to plasticity and sprouting of spared axons at the lesion site.[17] Implantation of a biomaterial bridge provides the opportunity to manipulate this host response observed in contusion and compression injuries. Bridges that are highly porous have been reported to support host cell infiltration that limits cyst formation.[5,18,19] Furthermore, many bridges have channels that support directed axonal growth into and through the injury.[5,20]

In this report, our objective was to characterize the dynamic host response following SCI to an implanted biomaterial bridge and regeneration in terms of the number and types of axons entering the bridge for more than 6 months following implantation. A 6-month time course represents a comprehensive time period that includes the acute and the chronic response as well as time points before, during, and after bridge degradation, which has not been previously characterized for bridges. A porous, degradable, multiple channel bridge, with an interconnected porous structure, was implanted in a rat thoracic spinal cord lateral hemisection injury model immediately postinjury. The number of axons was quantified at multiple time points in the rostral, middle, and caudal regions of the bridge, with staining to assess whether ascending and descending fibers were present. Furthermore, we investigated myelination of these axons by endogenous oligodendrocytes and infiltrating Schwann cells as a function of the channel location. Finally, the extracellular matrix (ECM) composition was characterized overtime. Histological analysis was used to characterize the dynamic host response from the time of bridge implantation to after complete degradation and is essential to identify targets for subsequent intervention to promote regeneration.

Materials and Methods

Rat spinal cord hemisection injury model

Porous multiple channel bridges (Fig. 1b) were fabricated by a gas foaming/particulate leaching method as previously described.[19,21,22] A rat spinal cord hemisection injury model was applied to analyze the host response to the implanted bridge. Surgery was performed as previously described[19,22,23] on female Long-Evans rats (180–200 g; Charles River) that were treated according to the Animal Care and Use Committee guidelines at the Northwestern University and the University of California Irvine. Animals were deeply anesthetized using isoflurane (3% in O_2), and a T9-T10 laminectomy was performed to expose the spinal cord. A 4-mm-long hemisection lateral of midline was removed, and the bridges were implanted in the injury space and covered by Gelfoam (Fig. 1). The muscles were sutured, and the skin was stapled. Postoperative care consisted of the administration of Baytril (enrofloxacin 2.5 mg/kg SC, once a day for 2 weeks), buprenorphine (0.01 mg/kg SC, twice a day for 2 days), and lactate ringer solution (5 mL/100 g, once a day for 5 days). Bladders were expressed twice daily until bladder function recovered (7–14 days).

Histological procedures

Spinal cord tissue was collected at 1, 2, 4, 6, 8, 9 weeks, and 6 months postimplantation with $n \geq 3$ at each time point. Rats were euthanized and spinal cord segments were snap frozen in isopentane and embedded (OCT; Sakura Finetek). Cords were sectioned either transversely or longitudinally to the long axis of the bridge in 12-μm-thick sections.

Immunostaining

Neurofilament, choline acetyltransferase, calcitonin gene-related peptide, and CS-56. Tissue sections were postfixed in 4% paraformaldehyde (PFA) for 15 min, and endogenous peroxide was blocked with 0.3% hydrogen peroxide in methanol for 30 min. Primary antibodies used were NF200 (1:5000; Sigma-Aldrich N4142), calcitonin gene-related peptide (CGRP, 1:10,000; Chemicon AB5920), choline acetyltransferase (ChAT, 1:200; Chemicon AB5042), and CS-56 (1:2000; Sigma-Aldrich C8035). The secondary antibody used for these stains was biotin-SP-conjugated AffiniPure F(ab)'2 donkey anti-rabbit (1:250; Jackson 711-066-152) except for CS-56 when a biotinylated horse anti-mouse (1:200; Vector BA2001) was used. Slides were incubated with an avidin:biotin enzyme complex (ABC Kit; Vector SK6100) and developed with DAB (Vector SK-4100) or for ChAT with NovaRed (NovaRED Kit; Vector SK4800).

ECM proteins. For collagen, tissues were fixed in prechilled acetone for 10 min and then incubated in primary antibody overnight at 4°C. The primary antibodies used were anti-rat collagen I (1:75; Sigma SAB4500362) or anti-rat collagen IV (1:500; Abcam ab6586), and the secondary antibody used for both was Alexa Fluor 555 goat anti-rabbit (1:500; Invitrogen A21424).

For laminin and fibronectin, tissues were fixed for 12 min in 4% PFA, washed with phosphate-buffered saline (PBS), and then incubated as above. The primary antibodies used were anti-rat laminin (1:500; Sigma-Aldrich L9393) or anti-rat fibronectin (1:250; Millipore AB2040), and the secondary antibody used for both was Alexa Fluor 555 goat anti-rabbit IgG (1:500; Invitrogen A21424). For laminin, 0.5% Triton-X100 in PBS was used to dilute the primary antibody and for washes. For all ECM proteins, four tissues from two animals were stained for analysis.

MBP/P0/NF200 triple staining

Tissues were fixed for 30 min in prechilled methanol, dehydrated, and rehydrated in graded ethanol and washed with PBS. Slides were incubated in a blocking solution for 1 h (1:20 BlockHen II, Aves BH-1001 in 5% normal goat serum in PBS) and washed with 0.1% Tween-20 in PBS. Simultaneous primary incubation was performed overnight at 4°C using the following primary antibodies: anti-p-zero myelin protein (1:100; Aves PZ0), anti-MBP (1:500; Millipore MAB382), and anti-NF200 (1:50; Sigma-Aldrich N4142). The secondary antibodies used were FITC goat anti-chicken IgY (1:500; Aves F1005), Alexa Fluor 546 goat anti-mouse (1:500; Invitrogen A11030), and Alexa Fluor 647 goat anti-rabbit (1:500; Invitrogen A21245). Fluorescence images were captured with a Photometrics CoolSNAP HQ2 camera using a Leica DMIRB microscope.

Axon quantification

Cords were retrieved for the quantification of axon numbers at 1 week ($n=3$), 2 weeks ($n=6$), 4 weeks ($n=6$), 6 weeks ($n=4$), 9 weeks ($n=4$), and 6 months ($n=3$). The bridge was divided into three regions based on location: rostral, middle, and caudal (Fig. 1). Three sections per animal located at 300 μm (rostral), 2000 μm (middle), and 3500 μm (caudal) from the rostral bridge/tissue boundary were stained for neurofilament. Axons were counted in channels at 40× by a blinded researcher.

Glial scar quantification

Cords were retrieved at 1 week ($n=6$), 2 weeks ($n=4$), 6 weeks ($n=2$), and 9 weeks ($n=4$) postimplantation, frozen, sliced longitudinally in 12-μm-thick sections. Every eighth tissue section was immunostained for CS-56. Images were captured using a Leica DFC290 camera and Leica DMIL microscope at 2.5× and stitched together using the stitching software, PTGui. Using ImageJ, the CS-56 immunopositive area directly rostral and caudal to the bridge was determined for eight tissue sections per animal. An average area was calculated for both locations at all time points.

Statistics

For multiple comparisons, pairs were compared using an ANOVA with *post hoc* Bonferroni test with a p-value <0.05 defined as significant. The error bars represent standard errors.

Results

Temporal and spatial characterization of axon growth within the bridge

Multiple channel poly(lactide-*co*-glycolide) (PLG) bridges (Fig. 1a) were implanted in a rat spinal cord hemisection (Fig. 1b) to investigate the dynamics of axon growth into and through the bridge. The average axon number per channel was quantified in transverse sections at the rostral, middle, and caudal regions at indicated times (Fig. 1c). Neurofilament staining was localized overwhelmingly within the channels, suggesting that the channels orient axon growth and limit sporadic turning into the bridge pores (Fig. 2a).

The extent of axon growth increased significantly with time and was a function of bridge region (Fig. 2f). Few neurofilament positive axons were observed within the channels 1-week postsurgery (Fig. 2). Starting at 2 weeks, substantial numbers of axons were observed within the channels, with no significant difference between channels (data not shown). Axon number in the rostral region increased significantly at week 2 relative to week 1 but did not differ thereafter. Through 6 weeks, the average number of axons was lower in the middle of the bridge than in the rostral and caudal regions. At 2 weeks, the rostral and caudal regions had approximately 60 axons per channel, with only ~13 in the middle. At 6 weeks, the difference was smaller, yet still significant, with ~100 axons per channel in the rostral and caudal regions and ~35 in the middle region. In the middle region at 9 weeks, axon density was significantly greater than earlier times. Average axon density in the middle and caudal regions continued to increase from 9 weeks to 6 months. At 9 weeks, no significant differences were observed between any two regions. At 6 months, the rostral region had fewer axons than the middle and caudal regions, with no significant difference in axon number between the middle and caudal regions (Fig. 2). Additionally, after the bridge had fully degraded, at least five intact neurofilament bundles were observed within the regenerated tissue (Fig. 2b).

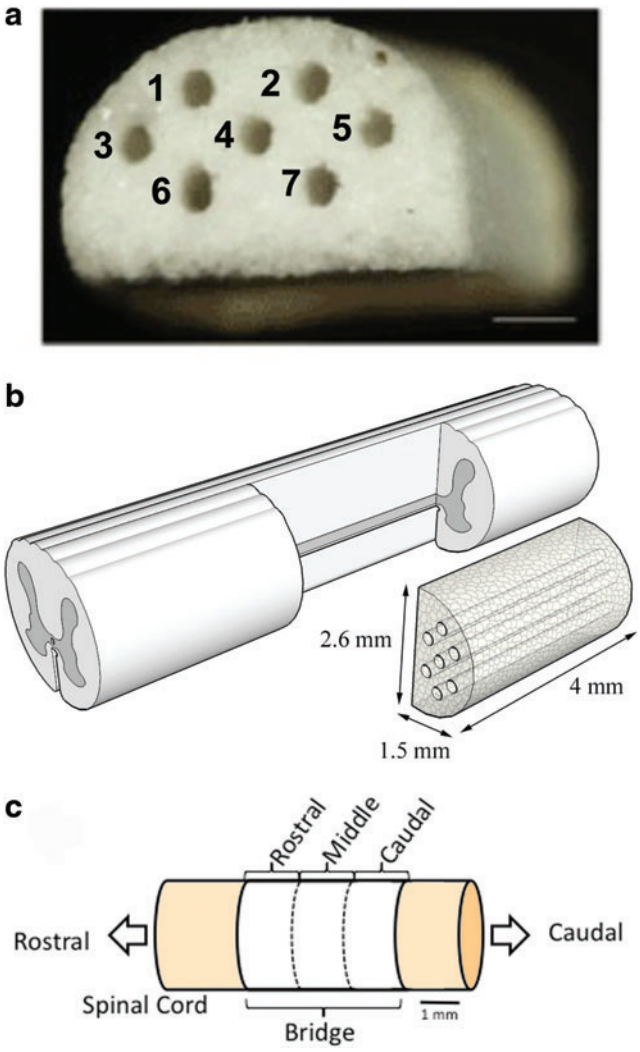

FIG. 1. Multiple channel bridges for spinal cord regeneration. **(a)** Photomicrograph of a multiple channel bridge showing seven channels, each 250 μm in diameter. Scale bar is 500 μm. **(b)** Schematic representation of PLG bridge implantation in a spinal cord hemisection. **(c)** Schematic representation of the regions in which the bridge was divided for analysis. Rostral analysis was performed at 300 μm, middle at 2000 μm, and caudal at 3500 μm from the rostral edge of the bridge/tissue boundary. Color images available online at www.liebertpub.com/tea

ChAT- and CGRP-positive axons within the channels

Longitudinal tissue sections were immunostained for motor and sensory axon markers. Long ChAT-positive axons were observed within the channels of the bridge (Fig. 3a). These ChAT-positive putative motor axons appeared in

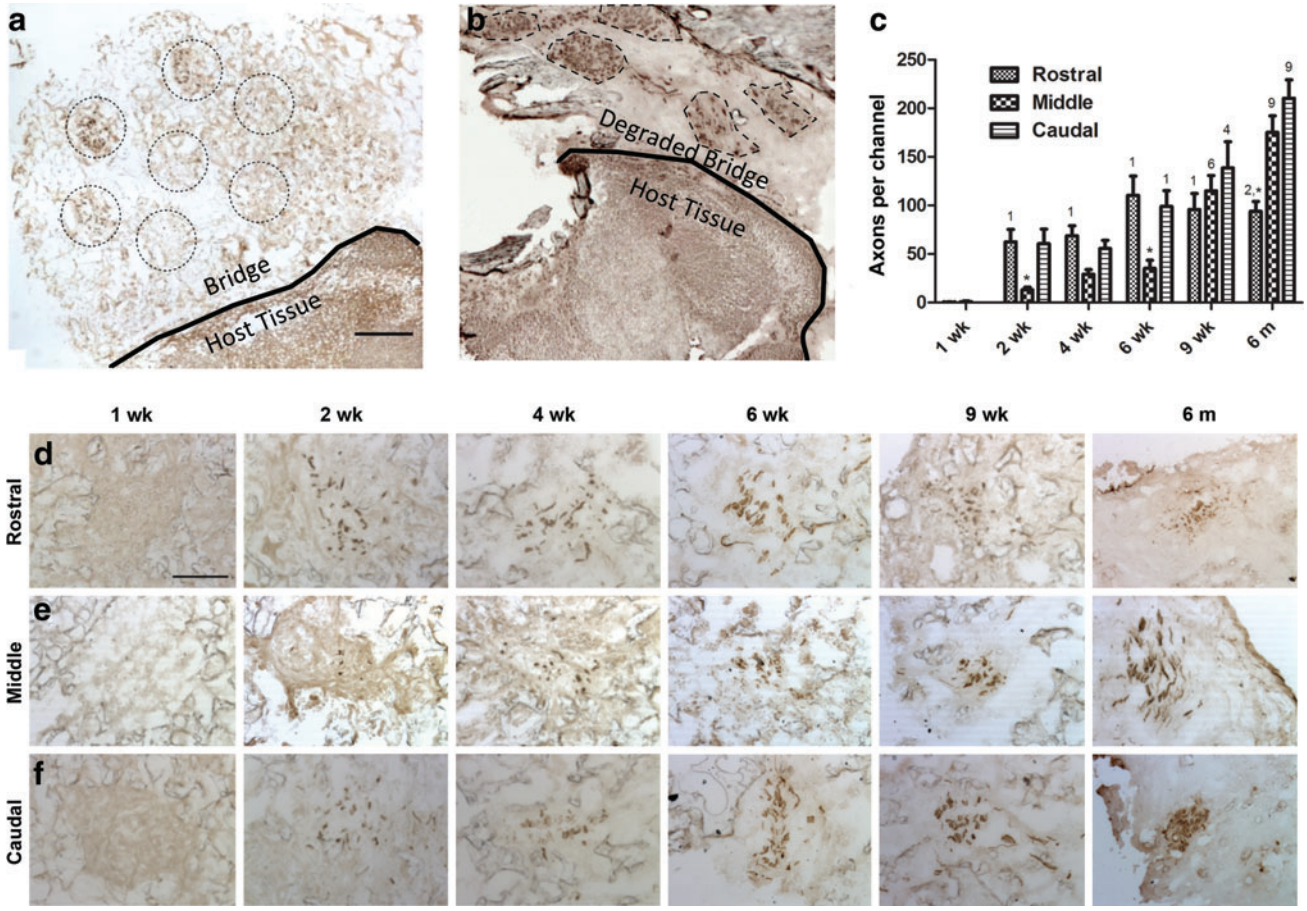

FIG. 2. Time course of axon growth in channels of the bridge. **(a)** NF200-stained cross section of the bridge at 9 weeks with seven channels indicated by dashed circles **(b)** NF200-stained cross section of the injury site at >6 months with a fully degraded bridge and at least five remaining neurofilament bundles outlined with dashes. Axons were stained at 1, 2, 4, 6, 9 weeks, and 6 months at **(c)** rostral (300 μm), **(d)** middle (2000 μm), and **(e)** caudal (3500 μm) regions of the bridge. **(f)** Quantification of axonal regeneration as a function of time and position within the bridges was performed by counting the number of NF200-positive axons inside the channels. Axon density was a function of time (ANOVA, $F = 56.8$, $p < 0.0001$) and location within the bridge (ANOVA, $F = 9.8$, $p < 0.0001$). Slides analyzed were selected from the NF200-stained cross sections as in **(c–e)**. Statistical analysis was carried out by an ANOVA with Bonferroni post-test with a $p < 0.05$ found to be significantly different. "*," significant difference compared to other locations at the same time point; "1, 2, 4, 6, 9," significant difference compared to 1, 2, 4, 6, and 9 weeks (respectively) and previous at the same location. Scale bar in **(a, b)** is 250 μm and in **(c–e)** is 50 μm. Color images available online at www.liebertpub.com/tea

bundles along the length of the channels. Sensory axons immunolabeled for CGRP were also present in the bridge channels (Fig. 3b). Qualitative observation suggested that fewer CGRP-stained axons were present in the channels relative to ChAT-labeled axons.

Myelination of axons within the channels

Myelination of axons and the source of myelination were subsequently investigated at 6-week and 6-month time points. An antibody against myelin basic protein (MBP) was used to identify all myelin (red), while an antibody against myelin protein zero (P0) was used to identify myelin from Schwann cells (blue) (Fig. 4). Sections were stained with NF200 to visualize axons (green) (Fig. 4). At 6 weeks, MBP was observed in several channels that contained regenerating axons (Fig. 4a). However, little to no P0 staining was observed at 6 weeks. In contrast, at 6 months, abundant MBP and P0 staining surrounding NF200-stained axons was observed throughout the bridge (Fig. 4b, c). MBP and P0 co-localized (purple) around axons in some areas, with other areas having only MBP or only P0 staining surrounding the axons (Fig. 4b). Generally, channels in the center of the bridge and near the midline of the spinal cord (channels 4, 6, and 7, Fig. 1a) had MBP-positive myelin without co-localization with P0. The channels located closer to the outer curved surface of the bridge had increased co-localization of MBP and P0 (Fig. 4b, c).

Temporal and spatial characterization of ECM molecules

Chondroitin sulfate proteoglycans. The glial scar is widely recognized as an inhibitor to regeneration[24–26]; thus, we subsequently characterized the dynamics of chondroitin sulfate proteoglycans (CSPGs) around the bridge. Longitudinal tissue sections from 1, 2, 6, and 9-week animals were immunostained for CS-56, which recognizes intact

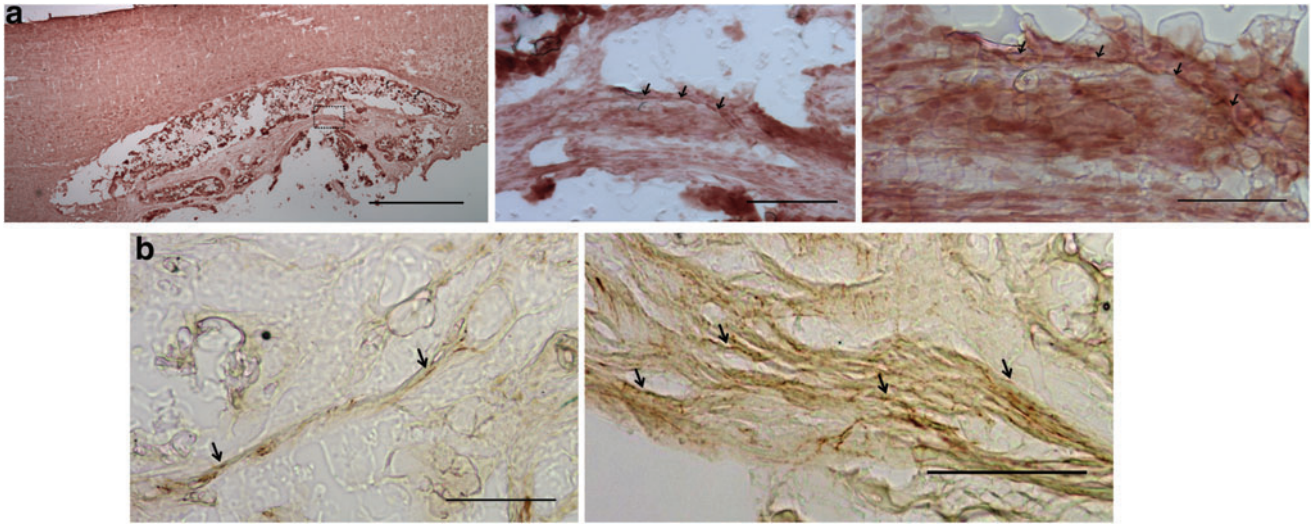

FIG. 3. Motor and sensory axons within channels of the bridge at 8 weeks. **(a)** ChAT-positive axons (red) within the channels of the bridge indicated by the arrowheads. Scale bars are 1000, 100, and 50 mm from left to right. **(b)** CGRP-positive axons (brown) within the channels of a bridge indicated by the arrows. Scale bars are 50 mm. Color images available online at www.liebertpub.com/tea

chondroitin-4-sulfate and chondroitin-6-sulfate proteoglycans.[27] The pattern of CS-56 labeling postinjury, far from the bridge, was similar to uninjured cord (Fig. 5a–f). CS-56 staining was strongest at the host/bridge interface at early time points (Fig. 5b) and declined overtime (Fig. 5b–e). CS-56 staining area was quantified at the rostral and caudal ends of the bridge, where axons enter and/or exit the channels. The CS-56-labeled area significantly decreased with time at both ends. By 6 weeks, the CS-56 area significantly decreased by more than twofold at the rostral end and almost threefold at the caudal end. This trend continued at 9 weeks with a greater than twofold decrease relative to 2 weeks in CS-56 area observed at both locations. No significant difference in CS-56 staining was observed between the rostral and caudal ends of the bridge at any time point (Fig. 5g).

Collagen IV and laminin. We subsequently investigated the distribution of laminin, which promotes axon growth, and collagen IV, which are upregulated following CNS injury and associated with fibrous scars and angiogenesis.[28] Immunostaining for collagen IV and laminin revealed similar patterns of expression postinjury (Figs. 6 and 7). Similar to CS-56 staining, the tissue far from the bridge was comparable to uninjured cord. At 1 week, dense positive staining was observed bordering the bridge, which corresponded to the CS-56-positive area, with little to no labeling inside the bridge (Figs. 5b, 6b, and 7b). The thickness of the collagen IV and laminin-positive border around the bridge decreased overtime. Starting at 2 weeks, collagen IV and, to a lesser degree, laminin labeling was observed within the bridge.

Collagen I and fibronectin. Collagen I and fibronectin are not principal components of the native CNS yet are involved in scar formation and can influence axon growth.[29] Thus, we characterized these factors at the implantation site. At 1 week, collagen I labeling increased slightly throughout the tissue and bridge, compared to uninjured tissue, with a thin positively stained border surrounding the bridge that

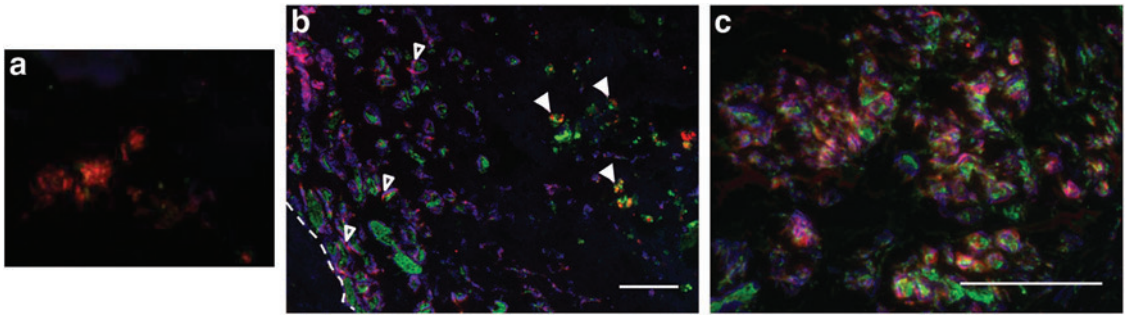

FIG. 4. Myelination of axons within the injury site overtime. Transverse tissue sections were stained with MBP (red), P0 (blue), and NF200 (green). **(a)** Cross section of a channel at 6 weeks stained positive for MBP but no P0 myelin. **(b, c)** At 6 months, extensive myelination was observed throughout the injury site. Co-localization of P0 and MBP myelin was observed around the outer curved surface of the bridge, indicated by open arrowheads in **(b)** and throughout in **(c)**. While mostly MBP, only myelin was observed toward the midline and center channels (numbered 4, 6, and 7 in Fig. 1a) indicated by the closed arrowheads in **(b)**. Scale bar is 100 μm. Color images available online at www.liebertpub.com/tea

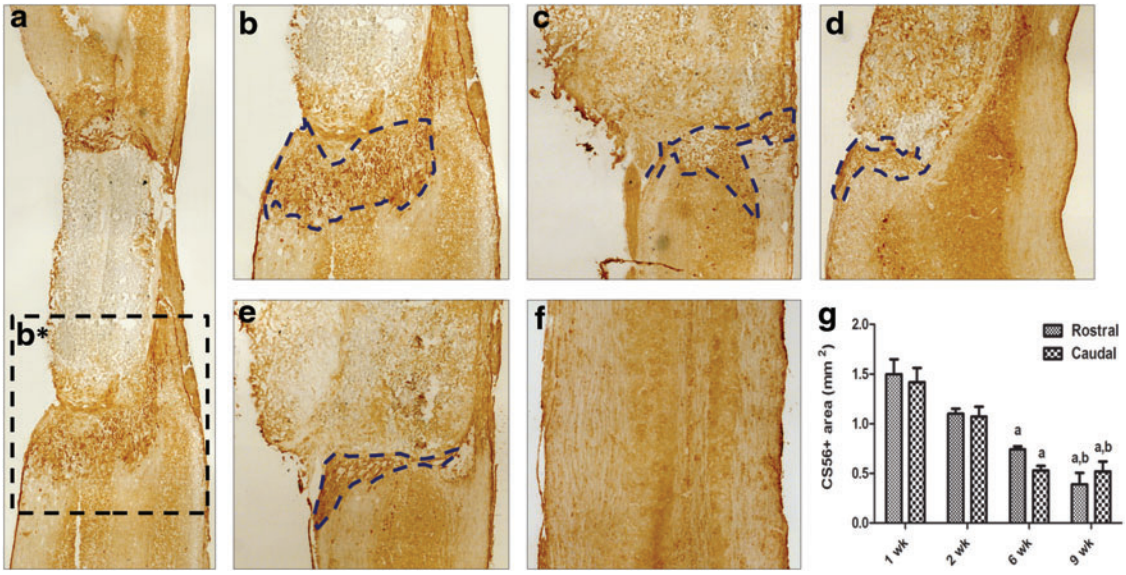

FIG. 5. Chondroitin sulfate proteoglycans (CSPG) staining over time. **(a)** CS-56-stained tissue section at 1 week with location of inset b* indicated by dashed lines. **(b–e)** Caudal sections at 1, 2, 6, and 9 weeks postimplantation with positive staining indicated by dashed lines. **(f)** Uninjured cord-negative control. **(g)** Quantification of the CS-56-positive area directly rostral and caudal to the bridge. "a," statistically different from 1 week at the same location; "b," statistically different from 2 weeks at the same location, $p < 0.05$. Color images available online at www.liebertpub.com/tea

disappeared by 9 weeks (Fig. 8). Positive collagen I staining was maximal within the bridge area at 2 to 6 weeks and decreased at 9 weeks.

Compared to uninjured spinal cord (Fig. 9a), at 1-week, diffuse positive staining for fibronectin was observed in tissue adjacent to and within the bridge area (Fig. 9b). Between weeks 2 and 9, this diffuse staining surrounding and in the bridge decreased (Fig. 9c–e). At 9 weeks, only a thin faint border of positive staining was visible around the bridge (Fig. 9e).

Discussion

In the present study, porous biodegradable PLG bridges containing seven channels with a diameter of 250 μm were implanted in a rat spinal cord hemisection injury. Bridge implantation prevented the formation of the fluid-filled cavity reported in rats after contusion injury. Structural integrity of the bridge was maintained through 9 weeks postimplantation, with the polymer borders visible for all seven channels. At 6 months, the polymer was completely degraded, and discrete individual bundles of axons were visible, consistent with an organization induced by the channels. Taken together, these bridges provided a structural support that initially guides regeneration and does not disrupt regenerated tissue through degradation.

The bridge supported robust axonal ingrowth into and across the bridge following implantation, consistent with other bridges. This axon growth indicates that the bridge tilts the balance of chemical and physical cues toward a more permissive environment, likely through physical support, secretion of trophic factors by host cells, and support from

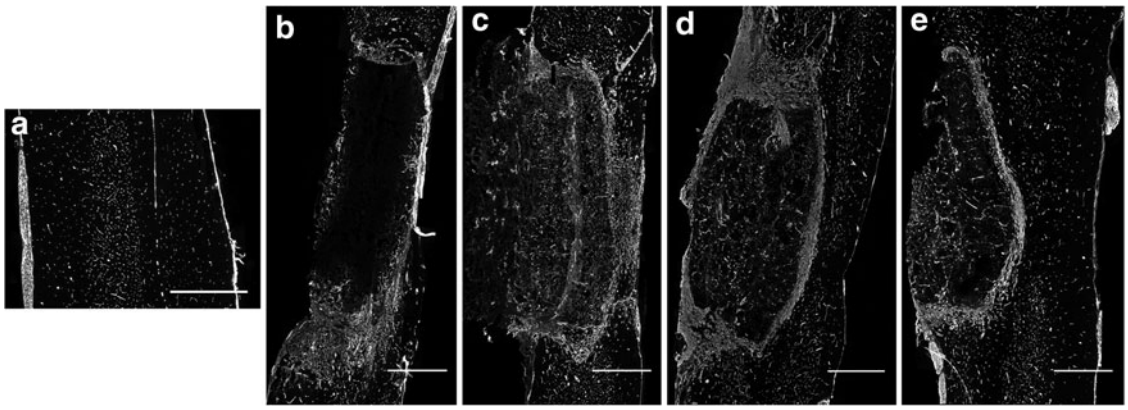

FIG. 6. Collagen IV-stained tissue sections of uninjured cord **(a)** and 1, 2, 6, and 9 weeks postimplantation **(b–e)**. Scale bar is 1 mm.

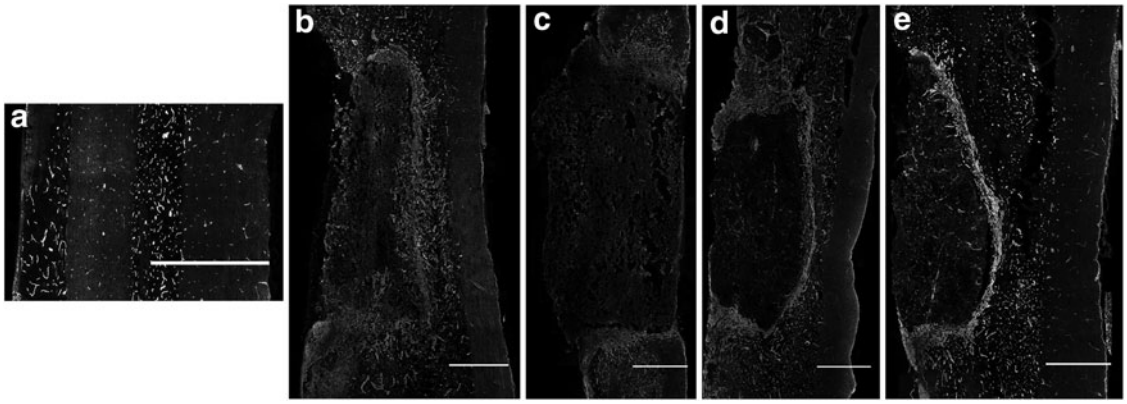

FIG. 7. Laminin-stained tissue sections of uninjured cord **(a)** and 1, 2, 6, and 9 weeks postimplantation **(b–e)**. Scale bar is 1 mm.

myelinating cells. Previous work indicates that the bridge's pores allow for infiltration of endogenous supportive cell types (i.e., Schwann cells, fibroblasts) that can express growth factors and deposit growth-promoting ECM, allowing long-term growth of axons.[19,22,23,30] The Oudega laboratory reported bridges formed by phase separation with longitudinally oriented macropores (75–300 μm) with varying lengths and degrees of interconnectedness.[31] These bridges were used in combination with either neurotrophins[31] or neurotrophins and Schwann cells.[32] Neurofilaments were observed near the rostral end, with few axons entering scaffolds from the caudal end,[31,32] and no significant directional growth across the bridge. The Yaszemski and Windebank collaboration has produced poly (lactic-*co*-glycolic) acid (PLGA) (85:15 co-polymer ratio) scaffolds with seven longitudinally oriented channels (450 μm diameter) formed by injection molding in conjunction with rapid solvent evaporation.[33–37] Their channels have interconnected pores with a controllable void fraction within 75–85%.[34] At 1 month postinjury, ~185 neurofilament-positive fibers were found within each 450 μm channel of Schwann cell seeded scaffolds, exceeding the numbers within 650 μm channels.[36] They have also used structurally similar bridges of oligo(polyethylene glycol) fumarate, which enhanced these numbers nearly twofold.[38] Bridges from other groups with similar longitudinal architectures fabricated from hydrogels (e.g., agarose,[39–41] pHEMA[42]) have provided directional alignment of axons, but these studies do not provide axonal counts or have minimal axonal ingrowth. Importantly, these other axon counts were calculated for bridges in conjunction with neurotrophin delivery or cell transplantation, which were not used in the present study. The number of regenerating axons reported herein is similar to the maximal number achieved with the other systems that also used additional measures. Considering axon density (axons/mm^2 of channel area), these bridges had a threefold higher density of neurofilament relative to Krych *et al.*[36]

In contrast to reports for these other bridge systems, the PLG bridges reported herein had an increasing number of axons following implantation through the 6-month time point (Fig. 2). Axon density was maximal at 6 months in the middle and caudal regions of the bridge, indicating that the axons are stable as the material degrades and suggesting some degree of functional synapse formation with interneurons or other targets that stabilizes the axons and prevents dieback.[43] Furthermore, axon survival after bridge degradation has been speculated to be a potential pitfall for biodegradable scaffolds. As the bridge degrades, the

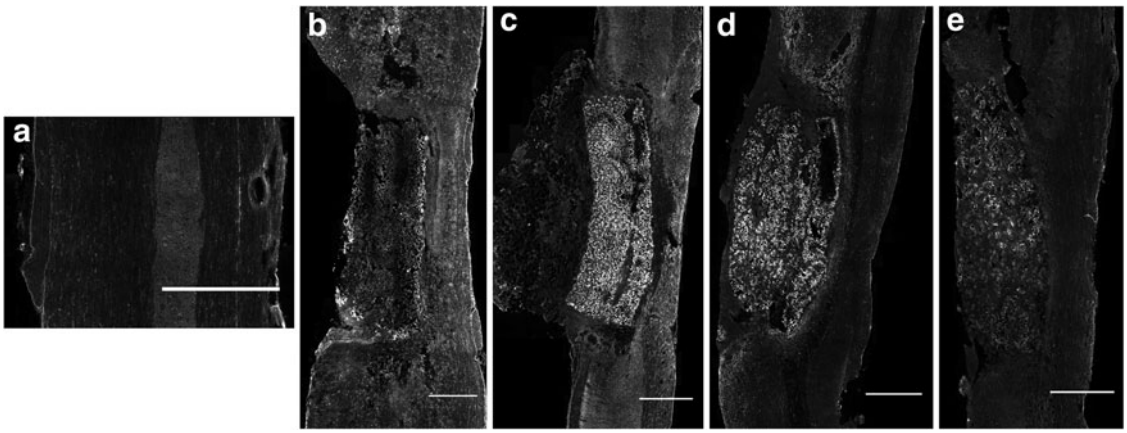

FIG. 8. Collagen I-stained tissue sections of uninjured cord **(a)** and 1, 2, 6, and 9 weeks postimplantation **(b–e)**. Scale bar is 1 mm.

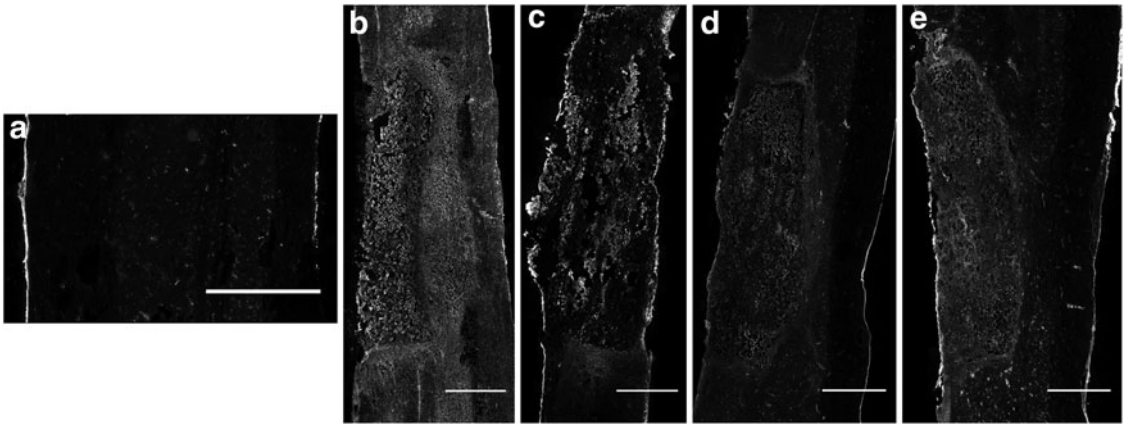

FIG. 9. Fibronectin-stained tissue sections of uninjured cord **(a)** and 1, 2, 6, and 9 weeks postimplantation **(b–e)**. Scale bar is 1 mm.

potential exists for damage to regenerated axons as their mechanical support is lost. Instead, we observed intact bundles of neurons at time points after bridge degradation, which supports the use of biodegradable bridges long-term and demonstrates the integration of the regenerated tissue with the host. While results from other studies are described, direct comparisons between bridges are complicated by differences in study design (such as surgical model) and endpoint analyses. The Oudega laboratory's bridge degraded between 4 and 6 weeks,[32] which may not have been sufficient to support the sustained presence of axons. The hydrogel bridges have not been investigated beyond 1 month. The bridges by Yaszemski and Windebank produced 185 axons per channel at 1 month, yet this count was reduced to ~80 by 2 months and remained at this level at 3 months.[36,38] Axons entering the caudal end were able to reenter the host tissue at the rostral end.[35] Their studies were performed in a transection model, which can retract relative to our hemisection model, and may lead to the reduction in axon counts. The thoracic lateral hemisection model used herein is a good model for investigating axon growth through the injury; however, this model is not appropriate for the analysis of functional recovery. Despite being performed in other studies, functional analysis was not performed herein as the thoracic hemisection model has significant plasticity and spontaneous recovery, disguising the source and degree of functional improvement. Taken together, the PLG bridges used herein were stable for at least 9 weeks and supported axon growth through the injury that increased throughout the study.

Both descending motor neurons and ascending sensory neurons extended axons into the bridge. Previous reports with bridges or peripheral nerve (PN) grafts indicated that a large percentage of the axons observed within the channels originated from neurons in the dorsal root ganglions (DRGs) adjacent to the bridge.[44,45] Since 66% of DRG neurons are CGRP positive in rodents,[46] the CGRP-positive axons within the channels likely originated from DRGs (Fig. 3b). However, a relatively small fraction of axons present within the bridge channels were CGRP positive, indicating that the majority of the axons originated from other neuron types. A portion of the axons in the channels at 8 weeks was identified as ChAT-positive putative motor neurons demonstrating a CNS origin of at least a percentage of the regenerated axons (Fig. 3a). Spontaneous compensatory sprouting of injured spinal motor systems occurs in the adult CNS and can result in functional recovery.[47,48]

Extensive myelination was observed at 6 months postimplantation as demonstrated by both positive MBP and positive P0 staining surrounding NF-positive axons. Demyelination and the lack of remyelination of regenerated axons are considered limiting factors in functional recovery. The extent of myelination was similar to previous reports,[23] yet the myelin source appears to shift over time from mostly MBP-positive and P0-negative at 6 weeks, indicating an oligodendrocyte origin, toward co-localization of MBP and P0 at 6 months, indicating a Schwann cell origin, particularly around outside the bridge. MBP only myelin staining was still observed in the bridge, near the midline, at 6 months. Both Schwann cell and oligodendrocyte remyelination have been associated with the recovery of saltatory conduction[49,50]; however, it is not yet known if both can promote axon survival[51,52] or carry signals across the injury. Multiple methods have been investigated to promote remyelination, including PN grafts or transplantation of Schwann cells or progenitor cells that can develop into oligodendrocytes to remyelinate axons.[44,53–56] Herein, we report extensive myelination by endogenous cells that migrated into the channels of the bridge, with myelination increasing through 6 months postinjury. While myelination is occurring, additional therapies that target oligodendrocyte recruitment or differentiation could further increase the extent of axon regeneration and remyelination.

CSPG staining at the bridge-tissue interface peaked at 1–2 weeks after injury and subsequently declined, consistent with studies in rat CNS.[57,58] Likewise, in contusion models, CSPGs normally surround the lesion.[59–62] Early deposition of CSPGs may limit the number of axons entering the bridge at early time points. The declining glial scar is consistent with our observations of increasing axon numbers with time. In a full transection injury model, bridges with channels of 440–660 μm diameter developed a fibrous scar-like rim inside each channel that was thicker and inhibited axon growth in the larger diameter channels,[36] a phenomenon not observed herein.

Collagen, laminin, and fibronectin are components of the fibrous scar that are deposited after injury to the CNS by cells

invading the bridge (e.g., Schwann cells, fibroblasts, macrophages).[19,23] The increase in ECM proteins and other scar components is similar to contusion injuries[15] and reflects the normal response to injury of reestablishing the CNS blood–brain barrier.[63] Laminin and fibronectin are axon growth promoting and have been used in various biomaterial implants for spinal cord regeneration.[29,64–69] Collagen IV and laminin deposition dynamics are consistent with reports of contusion injuries that indicate maximal staining 1–3 weeks postinjury.[28,63] Collagen I and fibronectin expression patterns were similar and correspond with infiltration of fibroblasts into the bridge, which have been reported to express these proteins after rat spinal cord contusions.[70]

Conclusion

In this report, we demonstrate that the bridge structure can support the growth of axons into an SCI. The bridge stabilizes the injury and prevents the formation of the fluid-filled cavity, common to contusion injuries.[71] In addition, we observed robust sustained axon growth with significant myelination out to beyond 6 months postimplantation when the bridge had completely degraded. Both putative sensory and motor axons were identified within the bridge, suggesting that CNS regeneration occurred. Decreasing levels of CSPGs surrounding the bridge suggest the potential to support axonal crossing. This characterization of the dynamic host response to the bridge suggests opportunities for combining additional therapies with implants to further enhance regeneration. Axon density and myelination are less within the bridge than in native uninjured tissue and could be increased with the delivery of neurotrophic factors.[23] However, even a small number of connections could result in significant gains in functional recovery.[4,72] The bridge supported improved regeneration beyond the limited spontaneous response to contusion injuries. Taken together, these results demonstrate the efficacy of a degradable multiple channel bridge to limit the inhibitory glial scar deposition and provide a permissive environment for long-term axon growth with myelination.

Acknowledgments

Financial support for this research was provided by the NIH (RO1 EB005678, R21 EB006520, RO1 EB003806). The authors thank the Christopher and Dana Reeve Foundation SCI core at UC Irvine.

Disclosure Statement

No competing financial interests exist.

References

1. Richardson, P.M., McGuinness, U.M., and Aguayo, A.J. Axons from CNS neurons regenerate into PNS grafts. Nature **284,** 264, 1980.
2. David, S., and Aguayo, A.J. Axonal elongation into peripheral nervous system "bridges" after central nervous system injury in adult rats. Science **214,** 931, 1981.
3. Geller, H.M., and Fawcett, J.W. Building a bridge: engineering spinal cord repair. Exp Neurol **174,** 125, 2002.
4. Joosten, E.A. Biodegradable biomatrices and bridging the injured spinal cord: the corticospinal tract as a proof of principle. Cell Tissue Res **349,** 375, 2012.
5. Wang, M., Zhai, P., Chen, X., Schreyer, D.J., Sun, X., and Cui, F. Bioengineered scaffolds for spinal cord repair. Tissue Eng Part B Rev **17,** 177, 2011.
6. Lonjon, N., Kouyoumdjian, P., Prieto, M., Bauchet, L., Haton, H., Gaviria, M., *et al.* Early functional outcomes and histological analysis after spinal cord compression injury in rats. J Neurosurg Spine **12,** 106, 2010.
7. Martin, D., Schoenen, J., Delree, P., Gilson, V., Rogister, B., Leprince, P., *et al.* Experimental acute traumatic injury of the adult rat spinal cord by a subdural inflatable balloon: methodology, behavioral analysis, and histopathology. J Neurosci Res **32,** 539, 1992.
8. Vanicky, I., Urdzikova, L., Saganova, K., Cizkova, D., and Galik, J. A simple and reproducible model of spinal cord injury induced by epidural balloon inflation in the rat. J Neurotrauma **18,** 1399, 2001.
9. Young, W. Spinal cord contusion models. Prog Brain Res **137,** 231, 2002.
10. Schwab, M.E., and Bartholdi, D. Degeneration and regeneration of axons in the lesioned spinal cord. Physiol Rev **76,** 319, 1996.
11. Zhang, S.X., Huang, F., Gates, M., White, J., and Holmberg, E.G. Histological repair of damaged spinal cord tissue from chronic contusion injury of rat: a LM observation. Histol Histopathol **26,** 45, 2011.
12. Beattie, M.S. Anatomic and behavioral outcome after spinal cord injury produced by a displacement controlled impact device. J Neurotrauma **9,** 157–9; discussion 9–60, 1992.
13. Zhang, S.X., Geddes, J.W., Owens, J.L., and Holmberg, E.G. X-irradiation reduces lesion scarring at the contusion site of adult rat spinal cord. Histol Histopathol **20,** 519, 2005.
14. Gledhill, R.F., Harrison, B.M., and McDonald, W.I. Demyelination and remyelination after acute spinal cord compression. Exp Neurol **38,** 472, 1973.
15. Zhang, S.X., Huang, F., Gates, M., and Holmberg, E.G. Scar ablation combined with LP/OEC transplantation promotes anatomical recovery and P0-positive myelination in chronically contused spinal cord of rats. Brain Res **1399,** 1, 2011.
16. Beattie, M.S., Bresnahan, J.C., Komon, J., Tovar, C.A., Van Meter, M., Anderson, D.K., *et al.* Endogenous repair after spinal cord contusion injuries in the rat. Exp Neurol **148,** 453, 1997.
17. Behrmann, D.L., Bresnahan, J.C., Beattie, M.S., and Shah, B.R. Spinal cord injury produced by consistent mechanical displacement of the cord in rats: behavioral and histologic analysis. J Neurotrauma **9,** 197, 1992.
18. Wong, D.Y., Leveque, J.C., Brumblay, H., Krebsbach, P.H., Hollister, S.J., and Lamarca, F. Macro-architectures in spinal cord scaffold implants influence regeneration. J Neurotrauma **25,** 1027, 2008.
19. De Laporte, L., Yang, Y., Zelivyanskaya, M.L., Cummings, B.J., Anderson, A.J., and Shea, L.D. Plasmid releasing multiple channel bridges for transgene expression after spinal cord injury. Mol Ther **17,** 318, 2009.
20. Yao, L., de Ruiter, G.C., Wang, H., Knight, A.M., Spinner, R.J., Yaszemski, M.J., *et al.* Controlling dispersion of axonal regeneration using a multichannel collagen nerve conduit. Biomaterials **31,** 5789, 2010.
21. De Laporte, L., Yan, A.L., and Shea, L.D. Local gene delivery from ECM-coated poly(lactide-co-glycolide) multiple channel bridges after spinal cord injury. Biomaterials **30,** 2361, 2009.
22. Yang, Y., De Laporte, L., Zelivyanskaya, M.L., Whittlesey, K.J., Anderson, A.J., Cummings, B.J., *et al.* Multiple channel

bridges for spinal cord injury: cellular characterization of host response. Tissue Eng Part A **15,** 3283, 2009.
23. Tuinstra, H.M., Aviles, M.O., Shin, S., Holland, S.J., Zelivyanskaya, M.L., Fast, A.G., *et al.* Multifunctional, multichannel bridges that deliver neurotrophin encoding lentivirus for regeneration following spinal cord injury. Biomaterials **33,** 1618, 2012.
24. Fawcett, J.W. Overcoming inhibition in the damaged spinal cord. J Neurotrauma **23,** 371, 2006.
25. Fitch, M.T., and Silver, J. CNS injury, glial scars, and inflammation: inhibitory extracellular matrices and regeneration failure. Exp Neurol **209,** 294, 2008.
26. Silver, J., and Miller, J.H. Regeneration beyond the glial scar. Nat Rev Neurosci **5,** 146, 2004.
27. Avnur, Z., and Geiger, B. Immunocytochemical localization of native chondroitin-sulfate in tissues and cultured cells using specific monoclonal antibody. Cell **38,** 811, 1984.
28. Loy, D.N., Crawford, C.H., Darnall, J.B., Burke, D.A., Onifer, S.M., and Whittemore, S.R. Temporal progression of angiogenesis and basal lamina deposition after contusive spinal cord injury in the adult rat. J Comp Neurol **445,** 308, 2002.
29. Cholas, R.H., Hsu, H.P., and Spector, M. The reparative response to cross-linked collagen-based scaffolds in a rat spinal cord gap model. Biomaterials **33,** 2050, 2012.
30. Bixby, J.L., and Harris, W.A. Molecular mechanisms of axon growth and guidance. Annu Rev Cell Biol **7,** 117, 1991.
31. Patist, C.M., Mulder, M.B., Gautier, S.E., Maquet, V., Jerome, R., and Oudega, M. Freeze-dried poly(D,L-lactic acid) macroporous guidance scaffolds impregnated with brain-derived neurotrophic factor in the transected adult rat thoracic spinal cord. Biomaterials **25,** 1569, 2004.
32. Hurtado, A., Moon, L.D., Maquet, V., Blits, B., Jerome, R., and Oudega, M. Poly (D,L-lactic acid) macroporous guidance scaffolds seeded with Schwann cells genetically modified to secrete a bi-functional neurotrophin implanted in the completely transected adult rat thoracic spinal cord. Biomaterials **27,** 430, 2006.
33. Friedman, J.A., Windebank, A.J., Moore, M.J., Spinner, R.J., Currier, B.L., and Yaszemski, M.J. Biodegradable polymer grafts for surgical repair of the injured spinal cord. Neurosurgery **51,** 742, 2002.
34. Moore, M.J., Friedman, J.A., Lewellyn, E.B., Mantila, S.M., Krych, A.J., Ameenuddin, S., *et al.* Multiple-channel scaffolds to promote spinal cord axon regeneration. Biomaterials **27,** 419, 2006.
35. Chen, B.K., Knight, A.M., de Ruiter, G.C.W., Spinner, R.J., Yaszemski, M.J., Currier, B.L., *et al.* Axon regeneration through scaffold into distal spinal cord after transection. J Neurotrauma **26,** 1759, 2009.
36. Krych, A.J., Rooney, G.E., Chen, B., Schermerhorn, T.C., Ameenuddin, S., Gross, L., *et al.* Relationship between scaffold channel diameter and number of regenerating axons in the transected rat spinal cord. Acta Biomater **5,** 2551, 2009.
37. Olson, H.E., Rooney, G.E., Gross, L., Nesbitt, J.J., Galvin, K.E., Knight, A., *et al.* Neural stem cell- and Schwann cell-loaded biodegradable polymer scaffolds support axonal regeneration in the transected spinal cord. Tissue Eng Part A **15,** 1797, 2009.
38. Chen, B.K., Knight, A.M., Madigan, N.N., Gross, L.A., Dadsetan, M., Nesbitt, J.J., *et al.* Comparison of polymer scaffolds in rat spinal cord: a step toward quantitative assessment of combinatorial approaches to spinal cord repair. Biomaterials 32, 8077, 2011.
39. Stokols, S., Sakamoto, J., Breckon, C., Holt, T., Weiss, J., and Tuszynski, M.H. Templated agarose scaffolds support linear axonal regeneration. Tissue Eng **12,** 2777, 2006.
40. Stokols, S., and Tuszynski, M.H. Freeze-dried agarose scaffolds with uniaxial channels stimulate and guide linear axonal growth following spinal cord injury. Biomaterials **27,** 443, 2006.
41. Stokols, S., and Tuszynski, M.H. The fabrication and characterization of linearly oriented nerve guidance scaffolds for spinal cord injury. Biomaterials **25,** 5839, 2004.
42. Yu, T.T., and Shoichet, M.S. Guided cell adhesion and outgrowth in peptide-modified channels for neural tissue engineering. Biomaterials **26,** 1507, 2005.
43. Eyre, J.A. Corticospinal tract development and its plasticity after perinatal injury. Neurosci Biobehav Rev **31,** 1136, 2007.
44. Nomura, H., Baladie, B., Katayama, Y., Morshead, C.M., Shoichet, M.S., and Tator, C.H. Delayed implantation of intramedullary chitosan channels containing nerve grafts promotes extensive axonal regeneration after spinal cord injury. Neurosurgery **63,** 127; discussion 41, 2008.
45. Richardson, P.M., McGuinness, U.M., and Aguayo, A.J. Peripheral nerve autografts to the rat spinal cord: studies with axonal tracing methods. Brain Res **237,** 147, 1982.
46. Hiruma, H., Saito, A., Ichikawa, T., Kiriyama, Y., Hoka, S., Kusakabe, T., *et al.* Effects of substance P and calcitonin gene-related peptide on axonal transport in isolated and cultured adult mouse dorsal root ganglion neurons. Brain Res **883,** 184, 2000.
47. Weidner, N., Ner, A., Salimi, N., and Tuszynski, M.H. Spontaneous corticospinal axonal plasticity and functional recovery after adult central nervous system injury. Proc Natl Acad Sci U S A **98,** 3513, 2001.
48. Zhou, L., Baumgartner, B.J., Hill-Felberg, S.J., McGowen, L.R., and Shine, H.D. Neurotrophin-3 expressed *in situ* induces axonal plasticity in the adult injured spinal cord. J Neurosci **23,** 1424, 2003.
49. Smith, K.J., Blakemore, W.F., and McDonald, W.I. Central remyelination restores secure conduction. Nature **280,** 395, 1979.
50. Blight, A.R., and Young, W. Central axons in injured cat spinal cord recover electrophysiological function following remyelination by Schwann cells. J Neurol Sci **91,** 15, 1989.
51. Zawadzka, M., Rivers, L.E., Fancy, S.P., Zhao, C., Tripathi, R., Jamen, F., *et al.* CNS-resident glial progenitor/stem cells produce Schwann cells as well as oligodendrocytes during repair of CNS demyelination. Cell Stem Cell **6,** 578, 2010.
52. Nave, K.A., and Trapp, B.D. Axon-glial signaling and the glial support of axon function. Annu Rev Neurosci **31,** 535, 2008.
53. Weidner, N., Blesch, A., Grill, R.J., and Tuszynski, M.H. Nerve growth factor-hypersecreting Schwann cell grafts augment and guide spinal cord axonal growth and remyelinate central nervous system axons in a phenotypically appropriate manner that correlates with expression of L1. J Comp Neurol **413,** 495, 1999.
54. Tuszynski, M.H., Weidner, N., McCormack, M., Miller, I., Powell, H., and Conner, J. Grafts of genetically modified Schwann cells to the spinal cord: survival, axon growth, and myelination. Cell Transplant **7,** 187, 1998.
55. Cummings, B.J., Uchida, N., Tamaki, S.J., Salazar, D.L., Hooshmand, M., Summers, R., *et al.* Human neural stem cells differentiate and promote locomotor recovery in spinal cord-injured mice. Proc Natl Acad Sci U S A **102,** 14069, 2005.

56. Keirstead, H.S., Morgan, S.V., Wilby, M.J., and Fawcett, J.W. Enhanced axonal regeneration following combined demyelination plus schwann cell transplantation therapy in the injured adult spinal cord. Exp Neurol **159,** 225, 1999.
57. Camand, E., Morel, M.P., Faissner, A., Sotelo, C., and Dusart, I. Long-term changes in the molecular composition of the glial scar and progressive increase of serotoninergic fibre sprouting after hemisection of the mouse spinal cord. Eur J Neurosci **20,** 1161, 2004.
58. Khaing, Z.Z., Milman, B.D., Vanscoy, J.E., Seidlits, S.K., Grill, R.J., and Schmidt, C.E. High molecular weight hyaluronic acid limits astrocyte activation and scar formation after spinal cord injury. J Neural Eng **8,** 046033, 2011.
59. Asher, R.A., Morgenstern, D.A., Shearer, M.C., Adcock, K.H., Pesheva, P., and Fawcett, J.W. Versican is upregulated in CNS injury and is a product of oligodendrocyte lineage cells. J Neurosci **22,** 2225, 2002.
60. Asher, R.A., Morgenstern, D.A., Fidler, P.S., Adcock, K.H., Oohira, A., Braistead, J.E., *et al.* Neurocan is upregulated in injured brain and in cytokine-treated astrocytes. J Neurosci **20,** 2427, 2000.
61. Moon, L.D., Asher, R.A., Rhodes, K.E., and Fawcett, J.W. Relationship between sprouting axons, proteoglycans and glial cells following unilateral nigrostriatal axotomy in the adult rat. Neuroscience **109,** 101, 2002.
62. Tang, X., Davies, J.E., and Davies, S.J. Changes in distribution, cell associations, and protein expression levels of NG2, neurocan, phosphacan, brevican, versican V2, and tenascin-C during acute to chronic maturation of spinal cord scar tissue. J Neurosci Res **71,** 427, 2003.
63. Stichel, C.C., and Muller, H.W. The CNS lesion scar: new vistas on an old regeneration barrier. Cell Tissue Res **294,** 1, 1998.
64. Houweling, D.A., Lankhorst, A.J., Gispen, W.H., Bar, P.R., and Joosten, E.A. Collagen containing neurotrophin-3 (NT-3) attracts regrowing injured corticospinal axons in the adult rat spinal cord and promotes partial functional recovery. Exp Neurol **153,** 49, 1998.
65. Yoshii, S., Oka, M., Shima, M., Taniguchi, A., Taki, Y., and Akagi, M. Restoration of function after spinal cord transection using a collagen bridge. J Biomed Mater Res A **70,** 569, 2004.
66. Cheng, H., Huang, Y.C., Chang, P.T., and Huang, Y.Y. Laminin-incorporated nerve conduits made by plasma treatment for repairing spinal cord injury. Biochem Biophys Res Commun **357,** 938, 2007.
67. King, V.R., Henseler, M., Brown, R.A., and Priestley, J.V. Mats made from fibronectin support oriented growth of axons in the damaged spinal cord of the adult rat. Exp Neurol **182,** 383, 2003.
68. Phillips, J.B., King, V.R., Ward, Z., Porter, R.A., Priestley, J.V., and Brown, R.A. Fluid shear in viscous fibronectin gels allows aggregation of fibrous materials for CNS tissue engineering. Biomaterials **25,** 2769, 2004.
69. King, V.R., Phillips, J.B., Hunt-Grubbe, H., Brown, R., and Priestley, J.V. Characterization of non-neuronal elements within fibronectin mats implanted into the damaged adult rat spinal cord. Biomaterials 27, 485, 2005.
70. Okada, M., Miyamoto, O., Shibuya, S., Zhang, X., Yamamoto, T., and Itano, T. Expression and role of type I collagen in a rat spinal cord contusion injury model. Neurosci Res **58,** 371, 2007.
71. Sroga, J.M., Jones, T.B., Kigerl, K.A., McGaughy, V.M., and Popovich, P.G. Rats and mice exhibit distinct inflammatory reactions after spinal cord injury. J Comp Neurol **462,** 223, 2003.
72. Bregman, B.S., Kunkel-Bagden, E., Schnell, L., Dai, H.N., Gao, D., and Schwab, M.E. Recovery from spinal cord injury mediated by antibodies to neurite growth inhibitors. Nature **378,** 498, 1995.

Address correspondence to:
Lonnie D. Shea, PhD
Department of Chemical Engineering
Northwestern University
2145 Sheridan Rd./Tech E156
Evanston, IL 60208-3120

E-mail: l-shea@northwestern.edu

Received: February 12, 2013
Accepted: October 15, 2013
Online Publication Date: December 10, 2013